# Radar Characteristics of Tropical Convection Observed During GATE: Mean Properties and Trends Over the Summer Season[1]

ROBERT A. HOUZE, JR., AND CHEE-PONG CHENG

*Department of Atmospheric Sciences, University of Washington, Seattle 98195*

(Manuscript received 4 February 1977, in revised form 2 May 1977)

ABSTRACT

Radar echo patterns observed daily during GATE have been analyzed to determine their mean characteristics and variations over the summer season. The characteristics analyzed were average echo areas, maximum heights, durations, number of high-intensity cores, motions, formation and dissipation modes, and orientations of echo lines.

As in tropical convective echo patterns in other parts of the world, small echoes ($<10^2$ km$^2$ area) dominated the total number of echoes while large echoes ($>10^3$ km$^2$ area) accounted for most of the area covered by precipitation. Echo height, duration and number of embedded cores were all positively correlated with echo area, and the most intense echo cores were found in the largest echoes, indicating that echo regions $>10^4$ km$^2$ in area were the areas of most enhanced convection. Echo areas, heights and durations tended to be log-normally distributed.

During late summer, the convection in large echoes ($>10^4$ km$^2$ area) was enhanced, showing greater vertical development as well as more numerous and more intense embedded cores than earlier in the summer.

Lower tropospheric winds appeared to control echo motions and played a role in the horizontal alignment of echo lines.

## 1. Introduction

The *Plan for U. S. Participation in the GARP Atlantic Tropical Experiment* (GATE) (National Academy of Sciences, 1971) stated that, "The central unsolved problem for the tropics is the mechanism or mechanisms by which deep cumulus convection is organized in the Interpropical Convergence Zone and the synoptic-scale convergence zones, waves, and vortices over the tropical oceans." The collective effects of large groups of convective clouds on the large-scale tropical environment thus formed the primary focus of GATE observations, and analysis of the data, now underway, is being directed toward elucidating the structure and processes associated with the cloud clusters observed in the experiment. Descriptions and diagnostic studies of GATE data are first steps leading toward an understanding of convection in the tropics and its interaction with large-scale flow.

Our study describes the mean characteristics of tropical cloud populations shown by GATE weather radar observations. The capability of weather radar to detect the intensity and three-dimensional structure of the precipitation beneath the large cloud shields seen in satellite pictures makes it an especially effective tool for describing the structure of tropical cloud systems. Previously, Iwanchuk (1973, hereafter referred to as IW) and López (1976, hereafter referred to as L) have described the radar characteristics of cloud systems over the western tropical Atlantic Ocean. The GATE radar data provide us with an opportunity to perform similar analyses of the radar characteristics of convection in the eastern tropical Atlantic Ocean, and this paper describes the results of our analysis of mean radar echo characteristics and their trends over the summer season covered by GATE.

The studies of IW and L were qualitative in the sense that they did not attempt to derive quantitative precipitation measurements from the radar data. However, they provided many useful measurements of echo sizes, shapes, duration and motions. Since these radar-observed quantities are closely related to cloud dynamics, their statistical distributions can provide physical insight for developing and refining models of cloud populations, such as those of Yanai *et al.* (1973), Austin and Houze (1973), Houze (1973), López (1973), Ogura and Cho (1973), Johnson (1976) and Houze and Leary (1976). Our study deals with the statistical distribution of qualitative echo features shown by GATE radar data. Specifically we examine echo areas, heights, durations, number of high-intensity echo cores, motions, echo formation and dissipation modes, and orientations of echo lines.

Our statistics of these echo features provide a framework in which to establish the representativeness of individual cloud systems chosen for intensive case

[1] Contribution No. 426, Department of Atmospheric Sciences, University of Washington.

studies. This statistical survey was accomplished relatively quickly since the qualitative echo features which we describe are not dependent on the time-consuming radar intercomparisons, calibration studies and extensive data processing required for deriving rainfall measurements from the GATE radar data. Our study, therefore, is a predecessor to more quantitative ones involving radar-derived rainfall estimates. In these future studies, radar observations of cloud population characteristics will be used as input to calculations of the mass, heat and momentum transports by convective cloud groups using refined versions of the models of Austin and Houze (1973), Houze (1973) and Houze and Leary (1976).

## 2. Data and methods of analysis

Four weather radars were employed in GATE at the sites shown in Fig. 1. Data collected with these radars include calibrated radar reflectivity recorded both photographically and digitally on magnetic tape. The first GATE radar data to become available to researchers were time-lapse films of the *Oceanographer* radar (wavelength 5.3 cm, beam width 1.5°, peak power 2.5 kW) plan position indicator (PPI) displays, which included base-level (0.6° antenna elevation angle) scans every 5 min and a complete three-dimensional scan once every 15 min. The three-dimensional scan consisted of a series of complete azimuthal sweeps at a sequence of elevation angles ranging from 0.6° to 22°, in increments of ~2°. The *Oceanographer* radar system is described in more detail by Hudlow (1975a,b). A radar scanning procedure similar to that employed on board the *Oceanographer* was followed on board each of the radar-equipped ships indicated in Fig. 1.

Our statistical survey of GATE radar echoes was initiated as soon as the *Oceanographer* radar films became available and is based entirely on that data set. We have no reason to believe that a survey based on data from one of the other radars would differ substantially from ours. All days on which the *Oceanographer* radar was operative (a total of 44 days) were included in the study.

The *Oceanographer* PPI displays appearing in the photographic data were quantized into a series of intensity levels, with threshold corresponding to the minimum detectable signal (level 1), 31 dBZ (level 2), 39 dBZ (level 3), 47 dBZ (level 4) and 55 dBZ (level 5; very few echoes ever reached this intensity). The level 1 contour was range-corrected during Phase I of GATE. However, the range-correction was abandoned for Phases II and III when it was discovered that the range-normalization procedure was reducing the sensitivity of the scope displays to weak echoes (Hudlow, 1975a). As a result, the areas of level 1 echoes in Phase I were slightly underestimated in the photographic data. This underestimate, however, did not have much effect on our results, since in this statistical survey we assigned echoes to rather broad size categories and the slight underestimate of their area due to the range-correction procedure used in Phase I did not appear to have any effect on the assignment of echoes to these categories.

Our analysis was centered on the base-level PPI display obtained at 1200 GMT on each day that the

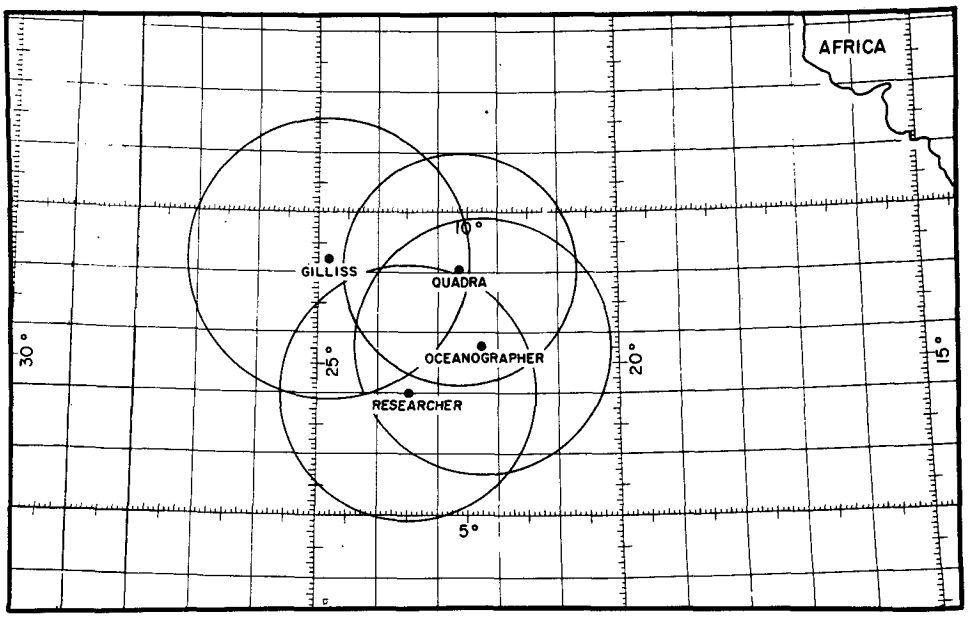


FIG. 1. Positions of ships (heavy dots) carrying quantitative weather radars during Phase III of GATE (late summer 1974). The Phase III ship positions do not differ much from those occupied during Phases I and II (early and mid-summer, respectively). Circles show the areas covered by each radar.

TABLE 1. Categories used in stratifying the tagged radar echoes observed at 1200 GMT on a given day. The area was determined at 1200 GMT. The height was the maximum attained by each echo during its lifetime.

| Area (km²) | Height (km) | Duration (min) |
|---|---|---|
| $A_1$ 0–100 | $H_1$ .5–1.3 | $D_1$ 5–25 |
| $A_2$ 100–200 | $H_2$ 1.3–2.1 | $D_2$ 25–50 |
| $A_3$ 200–300 | $H_3$ 2.1–2.9 | $D_3$ 50–75 |
| $A_4$ 300–400 | $H_4$ 2.9–3.7 | $D_4$ 75–100 |
| $A_5$ 400–500 | $H_5$ 3.7–4.5 | $D_5$ 100–125 |
| $A_6$ 500–600 | $H_6$ 4.5–5.3 | $D_6$ 125–150 |
| $A_7$ 600–700 | $H_7$ 5.3–6.1 | $D_7$ 150–175 |
| $A_8$ 700–800 | $H_8$ 6.1–6.9 | $D_8$ 175–200 |
| $A_9$ 800–900 | $H_9$ 6.9–7.7 | $D_9$ 200–225 |
| $A_{10}$ 900–$10^3$ | $H_{10}$ 7.7–8.5 | $D_{10}$ 225–250 |
| $A_{11}$ 1000–2000 | $H_{11}$ 8.5–9.3 | $D_{11}$ 250–275 |
| $A_{12}$ 2000–3000 | $H_{12}$ 9.3–10.1 | $D_{12}$ 275–300 |
| $A_{13}$ 3000–4000 | $H_{13}$ 10.1–10.9 | $D_{13}$ 300–325 |
| $A_{14}$ 4000–5000 | $H_{14}$ 10.9–11.7 | $D_{14}$ 325–350 |
| $A_{15}$ 5000–6000 | $H_{15}$ 11.7–12.5 | $D_{15}$ 350–375 |
| $A_{16}$ 6000–7000 | $H_{16}$ 12.5–13.3 | $D_{16}$ 375–400 |
| $A_{17}$ 7000–8000 | $H_{17}$ 13.3–14.1 | $D_{17}$ 400–425 |
| $A_{18}$ 8000–9000 | $H_{18}$ 14.1–14.9 | $D_{18}$ 425–450 |
| $A_{19}$ 9000–$10^4$ | $H_{19}$ 14.9–15.7 | $D_{19}$ 450–475 |
| $A_{20}$ >$10^4$ | $H_{20}$ 15.7–16.5 | $D_{20}$ 475–500 |
| | | $D_{21}$ 500–525 |

*Oceanographer* radar system was operative. Echoes at each intensity level threshold were tagged. In all over 2000 echoes were examined. The size of each tagged echo was measured by determining the lengths of its major and minor axes. Every echo, even if it was irregularly shaped, was fitted visually with a rectangle of equivalent area to determine its major and minor axes. The product obtained by multiplying the echo's major axis by its minor axis served as an estimate of the echo's area (denoted $A$). For each tagged echo, the number of higher intensity-level cores embedded within the echo and the orientation of the major axis were also recorded.

Each tagged echo present at 1200 GMT was tracked back and forth in time to determine its formation and dissipation modes, duration, velocity and maximum height attained during its lifetime. The formation and dissipation modes of each echo were classified as being either *independent* or due to echo *merger* or *splitting*.

The independent mode was one in which an isolated echo formed simply by appearing or dissipated simply by disappearing.

Merger refers to the union of two or more echoes in close proximity. Unions lasting only 15 min or less were considered chance, temporary colocations of echoes and not true mergers. If the smaller of two uniting echoes constituted at least one-fourth of the area of the echo produced by the union, and the union was maintained for more than 15 min, the new echo is said to have *formed by merger*, while the old echoes, which ceased to exist as separate entities after the merger, are said to have *dissipated by merger*. If a nontemporary union of two echoes involved an echo which had an area less than one-fourth of that of the echo produced by the union, it was assumed that, rather than producing a new echo, the union simply resulted in an incremental growth of the larger old echo which continued to exist. The smaller old echo, which lost its identity by being incorporated into the larger echo is, however, said to have dissipated by merger.

Splitting refers to the dissolution of an echo into two or more fragments. Dissolutions lasting only 15 min or less were considered temporary and not true splits. If the smaller of two echo fragments produced by a dissolving echo constituted at least one-fourth of the area of the echo prior to its dissolution and the dissolution was maintained for at least 15 min, the new echoes are said to have *formed by splitting*, while the old echo is said to have *dissipated by splitting*. If a nontemporary dissolution of an echo into two fragments resulted in an echo fragment which had an area less than one-fourth of that of the echo which dissolved, it was assumed that the original echo did not dissipate by splitting, but rather shrank by a small increment and continued to exist in the form of the larger fragment. The smaller fragment, however, was said to have formed by splitting.

The data tabulated for each tagged echo were stratified into categories of the echo's area at 1200 GMT, the maximum height it attained during its lifetime, and its duration (Table 1). Using these stratifications, we present results first in the form of averages and totals characterizing the echo population for the whole summer season in Section 3. Then in Section 4 changes in the convective population over the summer season are investigated by further stratifying our results according to the three official phases of GATE, corresponding to early, middle and late summer.

## 3. Characteristics of the average GATE echo population

### a. Horizontal dimension

In the early planning of GATE (e.g., see ISMG, 1972), it was recognized that tropical weather phenomena are usually composed of a hierarchy of horizontal scales, with synoptic-scale disturbances (thousands of kilometers in wavelength) containing cloud clusters ($10^2$–$10^3$ km in horizontal dimension), which, in turn, contain mesoscale precipitation areas ($10^1$–$10^2$ km in

TABLE 2. Scales of phenomena.

| Scale | Horizontal area (km²) | Descriptive term |
|---|---|---|
| A | >$10^6$ | Synoptic scale |
| B | $10^5$–$10^6$ | Cloud-cluster scale |
| B/C | $10^3$–$10^5$ | Mesoscale |
| C | $10^2$–$10^3$ | Mesoscale |
| D | 1–$10^2$ | Cumulus scale |

horizontal dimension). Cumulus-scale cores of convective activity (1–10 km in horizontal dimension) are found within the mesoscale precipitation areas. The nomenclature we use for describing the scales of phenomena in GATE (given in Table 2) is consistent with terminology adopted by GATE planners and is similar to the nomenclature used by L. Radar echoes examined in the present study were all D, C or B/C scale.

The relative frequency of D, C and B/C scale echoes in our data sample is shown in Fig. 2. The echo areas represented in Fig. 2 and in all of the statistical distributions presented hereafter in this paper were delineated by level 1 (minimum detectable threshold) contours, which outline as nearly as possible the entire extent of each separate precipitation region. Since the area covered by the *Oceanographer's* radar scope was $1.7 \times 10^5$ km$^2$, we expect that the measured areas of the largest B/C scale echoes were somewhat underestimated when these echoes extended beyond the range of the radar scope. A total of 1056 level 1 echoes were examined and included in this study. The stronger cores of precipitation, outlined by higher intensity thresholds within the level 1 echoes, are discussed in Section 3d.

From Fig. 2, it is seen that the GATE radar echo population was dominated by D scale echoes, which accounted for 67% of the level 1 echoes. C scale echoes also accounted for an appreciable proportion of the level 1 echoes (28%), while the very large B/C scale echoes accounted for only 8%. This type of distribution, dominated numerically by small echoes, is similar to that obtained by L, who pointed out that his distribution was "log-normal." That is, when plotted on log-probability paper, the distribution appeared as a straight line, indicating that the logarithm of echo size was normally distributed [for a thorough discussion of the log-normal distribution, see the book by Aitchison and Brown (1957)]. Biondini (1976) found that radar characteristics of clouds over Florida were log-normally distributed and in a more recent paper López (1977) has shown that radar echo heights, horizontal sizes and durations are log-normally distributed in a wide variety of convective situations.

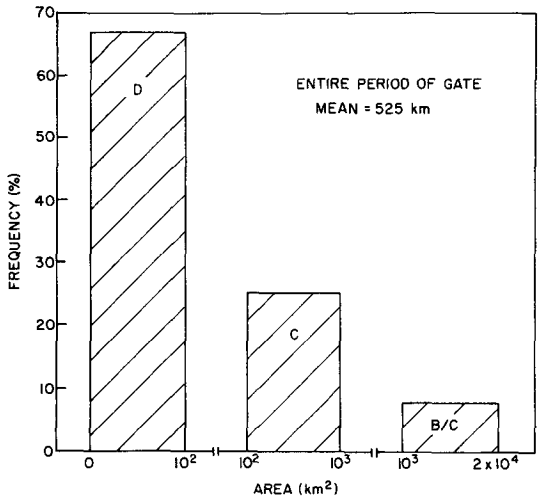


FIG. 2. Frequency of occurrence of D, C and B/C scale radar echoes during GATE.

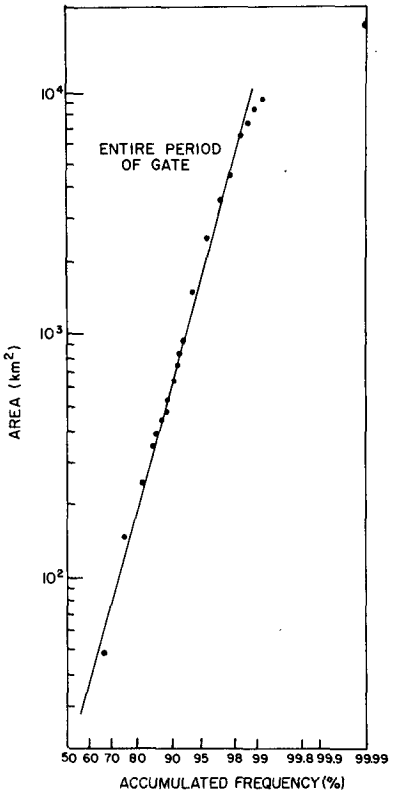


FIG. 3. Accumulated frequency distribution of areas covered by GATE radar echoes plotted in log-probability format. The straight line shows the log-normal distribution computed from the mean (1.54) and standard deviation (0.83) of the logarithms of the observed echo areas.

The GATE echo area distribution, shown in log-probability format in Fig. 3, also appears to be log-normal, with a deviation from a straight line noted only for echoes $> 10^4$ km$^2$ in area. These extremely large echoes, however, account for $< 1\%$ of the accumulated frequency. And it has been shown by López (1977) that this deviation from log-normality in the large-echo tail of the distribution is characteristic of a truncated log-normal distribution. We attribute the truncated shape of the frequency distribution of echo areas to the radar's range limit that underestimates the areas of the largest echoes when these extend far from the ship, and to the inherent space and time scales of tropical cloud clusters, which do not typically develop synoptic-scale areas of continuous cloud and precipitation. Application of the chi-square test for goodness of fit of the GATE radar observations to the straight line in Fig. 3 shows that the hypothesis that the observed distribution is log-normal for echoes $< 10^4$ km$^2$ in area

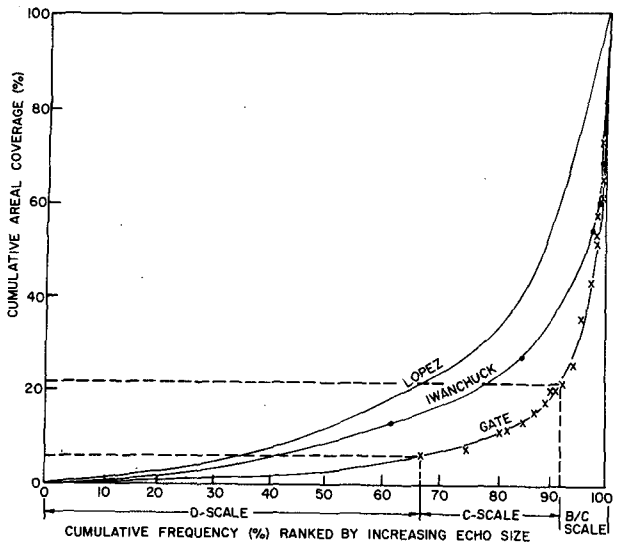


FIG. 4. Cumulative frequency distribution of accumulated echo areal coverage. Western tropical Atlantic distributions compiled by López (1976) and Iwanchuk (1973) are shown for comparison. Dashed lines are referred to in text.

cannot be rejected at the 5% level of significance. The log-normal tendency for GATE thus extends over a wider range of echo sizes than were investigated by L, whose largest echoes were 2100 km$^2$ in area.

While the similarity of our distribution to L's suggests a similarity between the convective regimes of the eastern and western Atlantic Ocean, much remains to be done concerning the physical interpretation of log-normal echo distributions. López (1976, 1977) discusses the possibility that their occurrence is the result of a multiplicative random process in which a step in the growth of an echo is a random proportion of its previous size.

From the dashed lines in Fig. 4, it can be seen that D scale echoes, which accounted for 67% of the total number of echoes in GATE (Fig. 2), covered only 5% of the total echo-covered area, and that D and C scale echoes, which accounted for 92% of the total number of echoes, covered only 21% of the total echo-covered area. The remaining 79% of the total area covered by echoes was covered by the B/C scale echoes. Hence, it is evident that the relatively few large precipitating areas present in tropical cloud populations take on great importance when their areal extent is considered. In Fig. 4, the GATE cloud population resembles those analyzed over the western Atlantic Ocean by both IW and L. Differences between our curve and theirs may be due to meteorological differences between the western and eastern Atlantic regions. However, they are more likely due to differences in the instrumentation used in each of the experiments. The sensitivity of the *Oceanographer* radar to light precipitation was quite high. Consequently, intense echo cores connected by light rain appearing as one large echo on the *Oceanographer* radar would appear as several smaller echoes on a less sensitive radar, with the result that a larger fraction of the total echo area would appear to be

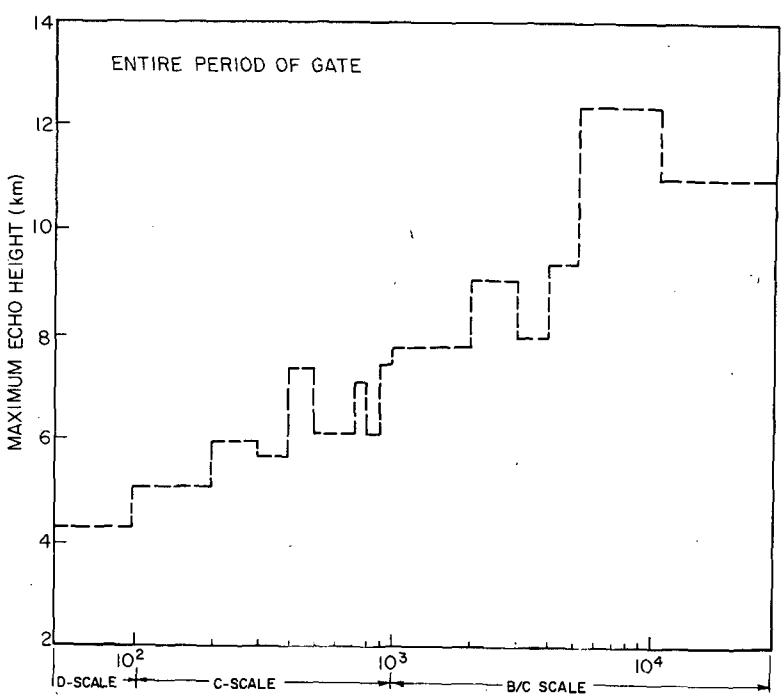


FIG. 5. Average maximum height of GATE radar echoes in different size ranges.

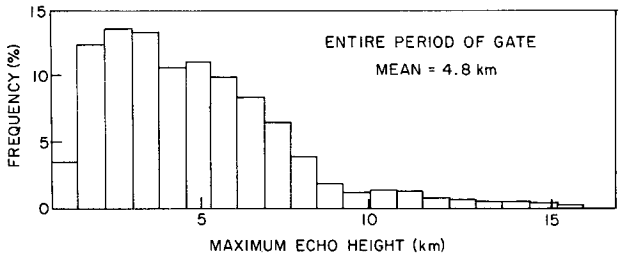


FIG. 6. Frequency distribution of the maximum heights of radar echoes observed ruring GATE. Arrow indicates mean value.

covered by smaller echoes, as indicated by IW and L in Fig. 4.

### b. *Echo height*

The average maximum height (AMH) of echoes in each of the area categories ($A_i$) listed in Table 1 was computed, and the resulting variation of AMH with $A_i$ is shown in Fig. 5. An almost linear increase in AMH with log $A_i$ is indicated. The average maximum heights of D, C and B/C scale echoes were 4.3, 5.8, and 9.9 km, respectively. The frequency distribution of maximum echo height is shown in Fig. 6. The mean value of maximum echo height in GATE, indicated in Fig. 6, was 4.8 km, which is within about 0.5 km of the average heights of the western Atlantic echoes studied by IW and L.

Plotted on log-probability paper, the GATE echo height distribution approximates a straight line, except in the largest few percent of the height categories where some deviation from a straight line is noted (Fig. 7). The portion of the observed distribution which approximates a straight line (i.e., the portion of the curve for heights <13 km) passes the chi-square test for goodness of fit to the log-normal distribution shown in Fig. 7 at the 5% level of significance. The deviation from log-normality for large echo heights seen in Fig. 7 was also noted by L and indicates the presence of fewer clouds than expected in a log-normal distribution. As pointed out by López (1977), this deviation is characteristic of a truncated log-normal distribution. Since convective clouds are limited by the height of the tropopause, their distribution is expected to be truncated at large heights.

TABLE 3. Formation and dissipation modes of GATE radar echoes. Numbers in parentheses indicate sample size.

| Mode of formation | D Scale | C Scale | B/C Scale |
|---|---|---|---|
| Independent | 74% | 42% | 2% |
| Merger | 5 | 22 | 59 |
| Splitting | 21 | 36 | 39 |
| | (235) | (275) | (85) |
| Mode of dissipation | | | |
| Independent | 74% | 36% | 12% |
| Merger | 21 | 37 | 39 |
| Splitting | 5 | 27 | 49 |
| | (238) | (270) | (78) |

### c. *Echo formation, dissipation and duration*

As explained in Section 2, each radar echo included in this study was tracked throughout its lifetime, and its formation and dissipation modes were identified. From Table 3, it can be seen that the smallest echoes (D scale) tended to form and dissipate independently, while the largest echoes (B/C scale) formed and dissipated primarily by mergers and splits. Similar results were found by L for the western Atlantic.

Echo duration was positively correlated with echo area coverage (Fig. 8). However, this relation was not as strong as that between area and height shown in Fig. 5. In Fig. 8, it can be seen that the durations of GATE

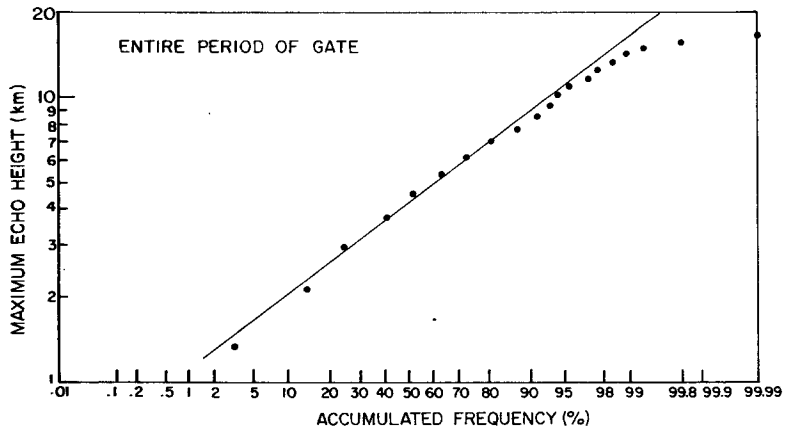


FIG. 7. Accumulated frequency distribution of the maximum heights of radar echoes observed during GATE plotted in log-probability format. The straight line shows the log-normal distribution computed from the mean (0.58) and standard deviation (0.21) of the logarithms of the observed maximum echo heights.

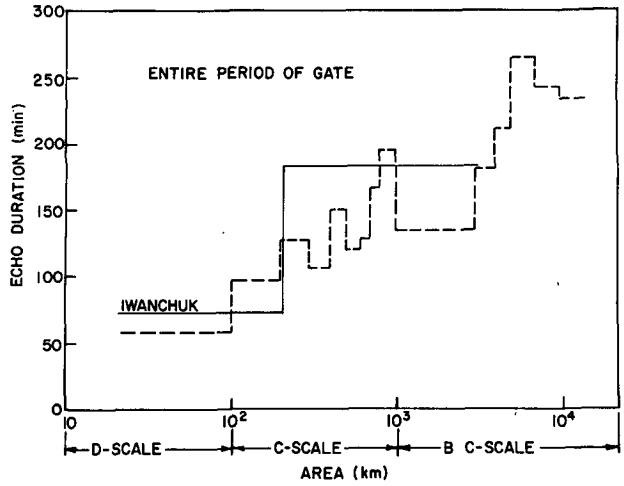


FIG. 8. Average durations of GATE radar echoes (dashed line) in different size ranges and values obtained by Iwanchuk (1973) for western tropical Atlantic echoes (solid line).

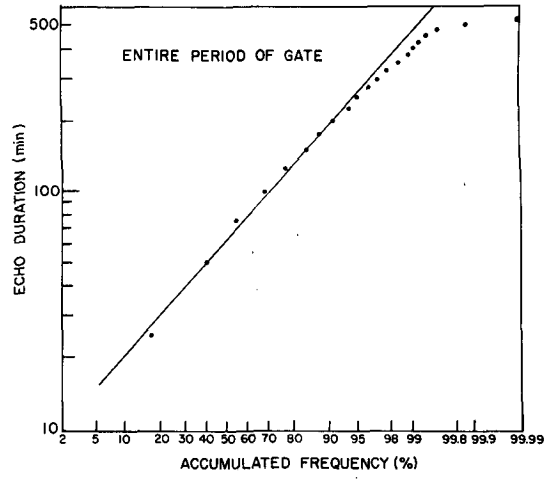


FIG. 10. Accumulated frequency distribution of GATE radar echo durations. plotted in log-probability format. The straight line shows the log-normal distribution computed from the mean (1.79) and standard deviation (0.38) of the logarithms of the observed echo durations in units of minutes.

echoes $<200$ km$^2$ in area agree quite closely with those observed over the western Atlantic Ocean by IW. However, for echoes with areas between 200 and 3000 km$^2$, the GATE echoes had durations which were shorter by a factor of $\sim$0.8. The shorter durations of the GATE echoes in this size range may be due to the fact that mergers and splits tended to truncate their lifetimes (Table 3).

The frequency distribution for echo duration is shown in Fig. 9 and in log-probability format in Fig. 10. From Fig. 10, it can be seen that echo durations were distributed log-normally, passing the chi-square test for goodness of fit to the straight line shown in Fig. 10 at the 5% level of significance for echo durations $<400$ min. This result is somewhat surprising since echo lifetimes were often truncated by mergers or splits. L found no tendency for the durations of echoes in the western Atlantic Ocean to be distributed log-normally; however,

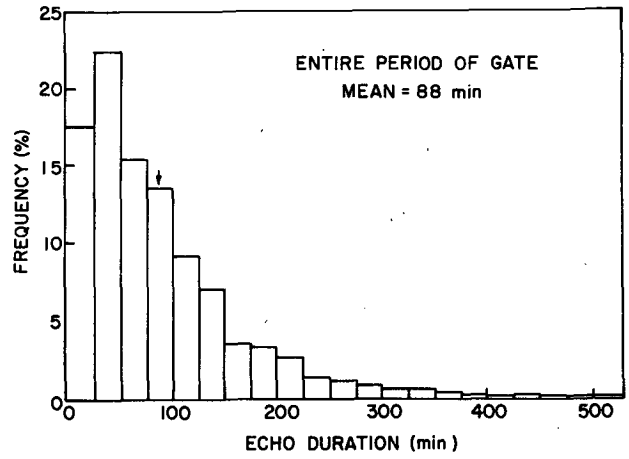


FIG. 9. Frequency distribution of GATE radar echo durations. Arrow indicates mean value.

in his later paper (López, 1977) he found that echo duration distributions in several other areas do follow a log-normal distribution.

*d. Echo internal structure*

An important question in modeling and understanding tropical convection concerns the extent to which large precipitating clouds contain smaller scale cores of relatively intense convection and rainfall. To address this question, we counted the number of higher intensity level cores (precipitation maxima) within each level 1 echo present at 1200 GMT for each day included in our study. Each core was classified as being a level 2, 3 or 4 core, depending on which was the highest threshold of radar reflectivity that was triggered. Level 4 cores were not counted again as level 3 or 2 cores, and level 3 cores were not counted as level 2 cores. Thus, no echo core was counted more than once. The results of our echo core survey are shown in Fig. 11.

It can be seen from Fig. 11 that multiple cores, i.e., more than one core per echo, were observed primarily in echoes larger than 500 km$^2$ in area (the B/C scale and larger C scales echoes). The results in Fig. 11 are based on the echo patterns at 1200 GMT each day and therefore indicate the average number of cores embedded in an echo of a given size at an instant of time. The possibility that an echo might have contained more cores which formed and dissipated in series over its lifetime is not precluded.

From Fig. 11, it is seen that the higher intensity cores (levels 3 and 4) were found predominantly in the very large B/C scale echoes. Echoes exceeding $10^4$ km$^2$ in area contained almost as many cores reaching levels 3 and 4 as were reaching level 2. The tendency for higher intensity cores to be found preferentially within the

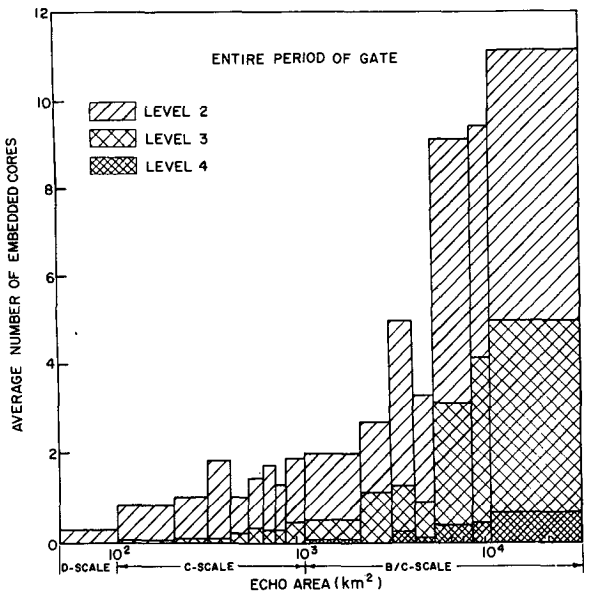


FIG. 11. Average number of embedded cores of maximum radar reflectivity located within GATE radar echoes in different size ranges. Shading indicates the fraction of the total number of cores in each size range which exceeded reflectivity threshold levels 2 (31 dBZ), 3 (39 dBZ) and 4 (47 dBZ).

B/C scale echoes indicates that these large echoes formed a favorable environment for the development of intense convective cores or that the more intense convention produced surrounding areas of widespread precipitation (possibly from anvil clouds).

IW determined the average number of cores in echoes ranging in maximum size from 200 to 300 km² in area and found that the average number of cores per echo was 4.8. From Fig. 11, it can be seen that this is about three times as many cores as we found in GATE echoes in the same size range. This difference may be explained by the fact that the radar used in IW's study had a narrower beam width than that used by the *Oceanographer* in GATE; therefore, all of the small echo cores actually present may not have been fully resolved with the *Oceanographer* radar. Future studies using the higher resolution *Gilliss* and *Quadra* radar data collected in GATE should resolve this question.

TABLE 4. Number of days on which *Oceanographer* radar echoes moved in a direction within 25° of the wind direction at the indicated levels. CNP indicates comparison not possible due to light winds or because too few echoes were tracked to establish a reliable direction.

| | Altitude | | | | | |
|---|---|---|---|---|---|---|
| | Surface | 850 mb | 850 and 700 mb | 700 mb | CNP | Other |
| Number of days | 5 | 18 | 4 | 1 | 16 | 1 |

### e. *Echo motion*

Average GATE echo speeds are summarized in Fig. 12. Echoes associated with rapidly moving tropical squall lines have been omitted since squall line speeds were considerably greater than the velocities of other echoes and are, therefore, not representative of the general echo population [GATE squall lines are described by Houze (1975, 1976, 1977)]. No systematic variation of echo speed with echo size can be identified in Fig. 12. Echoes of all sizes moved at typical speeds of 3–5 m s$^{-1}$.

The average direction of echo motion determined for 1200 GMT each day was compared with the directions of streamlines over the radar area on synoptic charts prepared during the operational period of GATE for the surface 850 and 700 mb levels.[2] The results of these comparisons, shown in Table 4, indicate that the

[2] These charts are available as "Information Products Prepared During the Experiment" through the *GATE Data Catalogue* published by the Environmental Data Service, NOAA, U. S. Dept. of Commerce, Washington, D. C.

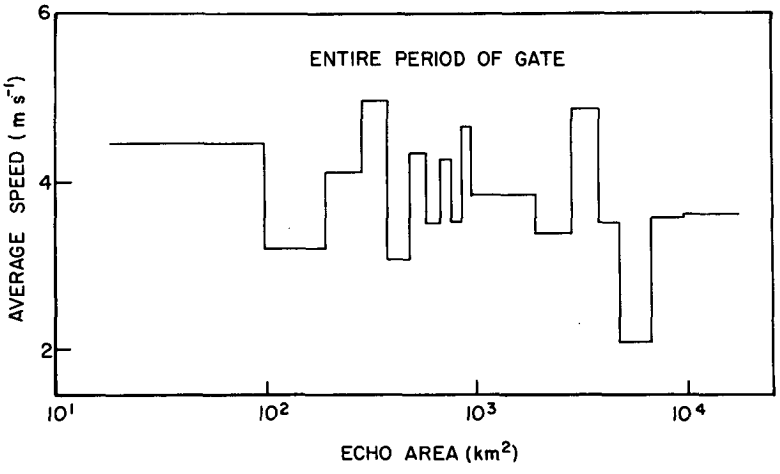


FIG. 12. Average speeds of GATE radar echoes in different size ranges.

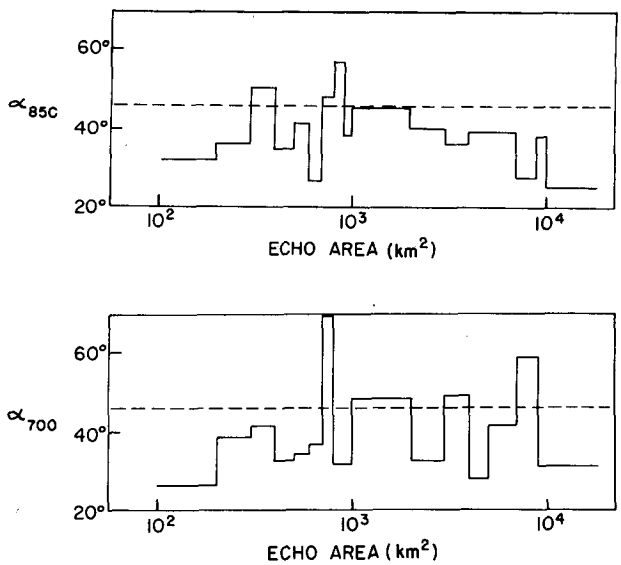


FIG. 13. Average acute angles ($\alpha_{850}$ and $\alpha_{700}$) formed by elongated radar echoes and the 850 and 700 mb streamlines, respectively. Dashed line at 45° indicates value expected for random echo orientations.

echoes were advected by the 850 mb wind on most occasions. This result is consistent with the findings of Pestaina-Haynes and Austin (1976) who tracked echo lines detected with the radar on the Canadian ship *Quadra* during GATE.

In obtaining the results in Table 4, it was found that echoes $<500$ km$^2$ in area moved erratically on about half of the days included in the study. However, when the small echoes ($<500$ km$^2$ in area) moved in a well-defined fashion, their motion was similar to that of the larger echoes ($>500$ km$^2$) in the same pattern. When the small echo motion was erratic, only the large echo motions were used in obtaining Table 4.

### *f. Orientation of echo lines*

About 83% of the C and B/C scale echoes appearing on the *Oceanographer* PPI at the level 1 intensity threshold were sufficiently elongated in the horizontal that they could easily be assigned an orientation. The orientations of these linear echoes were examined in relation to the wind field over the GATE area, as represented by the streamlines on the synoptic charts prepared during the experiment. A weak tendency for the linear echoes to be parallel to lower tropospheric winds is indicated in Fig. 13, which shows that the acute angles formed by the intersections of all elongated echoes in our data sample (total of 291) with the 850 and 700 mb streamlines tended to be less than 45°, the

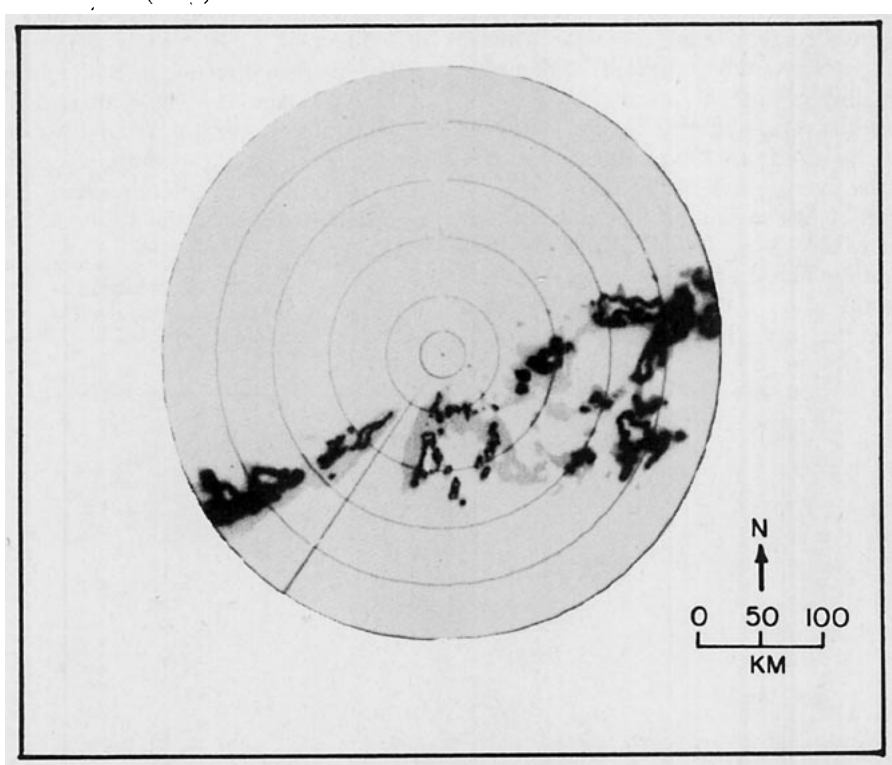


FIG. 14. Example of a group of radar echoes arranged in a line during GATE. Pattern shown is a photograph of the *Oceanographer* radar plan position indicator for 1145 GMT 12 August 1974. Shading thresholds are for minimum detectable signal (gray), 31 dBZ (black), 39 dBZ (white) and 47 dBZ (gray). Radial line indicates ship heading (a 20° sector was blocked by the ship's superstructure in this direction).

value expected for random echo orientations with respect to wind direction.

In addition to isolated echoes exhibiting linear shapes, it was also found that large groups of echoes tended to form in lines on 35 of the 44 days considered in this study (e.g., see Fig. 14). The orientations of these large echo group lines were more strongly related to the lower tropospheric wind field than were the orientations of isolated echoes. The echo group lines coincided (within ±25°) with the axes of surface confluent asymptotes on 16 occasions, which include every case in which both echo group lines and surface confluence lines existed in the vicinity of the *Oceanographer*. In 28 of the 35 cases in which echo group lines occurred, the echo line orientation agreed (within ±25°) with either the 850 mb wind (9 cases), 700 mb wind (12 cases) or both (7 cases).

From these comparisons, it is evident that both surface confluence and lower tropospheric wind direction are related to echo group orientation. However, neither factor appeared to be dominant. On twelve occasions, echo group lines occurred in the absence of a well-defined surface confluence line and on seven occasions the echo lines did not appear to be parallel to either the 850 or 700 mb wind. However, there were only two occasions on which there was no apparent relationship of echo group orientation to any of these features.

## 4. Changes in the GATE radar echo population over the summer season

Since GATE extended from 28 June to 19 September 1974, it is possible to examine temporal changes in the convective cloud population over the summer season. In this paper, we examine the seasonal trend by stratifying the *Oceanographer* radar data according to the three official phases of GATE. Echo patterns in early summer are characterized by 19 days of *Oceanographer* radar data from Phase I (28 June–16 July 1974), mid-summer patterns are indicated by 14 days of data from Phase II (28 July–15 August 1974), and late summer patterns by 11 days from Phase III (30 August–10 September 1974). *Oceanographer* radar data from the last half of Phase III were not used in this study because they were affected by an antenna-stabilization problem (Hudlow, 1975a). The number of level 1 echoes examined and included in our statistical distributions presented below is 488 for Phase I, 587 for Phase II and 181 for Phase III of GATE.

### *a. Horizontal dimensions*

From Fig. 15, it is evident that a considerably smaller fraction of D scale echoes and a larger fraction of C scale echoes were observed during Phase III of GATE than were present during Phases I and II. This changeover to a somewhat different convective regime later in the summer was probably related to the pronounced synoptic-scale wave activity during Phase III described by Reed *et al.* (1977).

Although the mean radar echo area increased as the summer progressed (Fig. 15), the shape of the echo area distribution was similar in all three phases of GATE. This can be seen in Fig. 16, where the distributions are shown in log-probability format. For all three phases, the echo-size distributions pass the chi-square test for goodness of fit to the log-normal distributions

TABLE 5. Formation and dissipation modes of radar echoes observed during each phase of GATE. Independent mode is indicated by I, merger by M, splitting by S. Numbers in parentheses indicate sample size.

| | Formation | | | Dissipation | | |
|---|---|---|---|---|---|---|
| Mode | D-scale echoes (%) | C-scale echoes (%) | B/C-scale echoes (%) | D-scale echoes (%) | C-scale echoes (%) | B/C-scale echoes (%) |
| Phase I | | | | | | |
| I | 85 | 52 | 6 | 72 | 46 | 3 |
| M | 2 | 21 | 61 | 23 | 37 | 58 |
| S | 13 | 27 | 33 | 5 | 17 | 39 |
| | (59) | (93) | (35) | (60) | (91) | (35) |
| Phase II | | | | | | |
| I | 71 | 46 | 0 | 73 | 36 | 22 |
| M | 6 | 18 | 45 | 20 | 33 | 22 |
| S | 23 | 36 | 55 | 7 | 31 | 56 |
| | (102) | (113) | (34) | (104) | (109) | (28) |
| Phase III | | | | | | |
| I | 68 | 23 | 0 | 77 | 24 | 13 |
| M | 7 | 29 | 81 | 19 | 40 | 27 |
| S | 25 | 48 | 19 | 4 | 36 | 60 |
| | (74) | (69) | (16) | (74) | (70) | (15) |

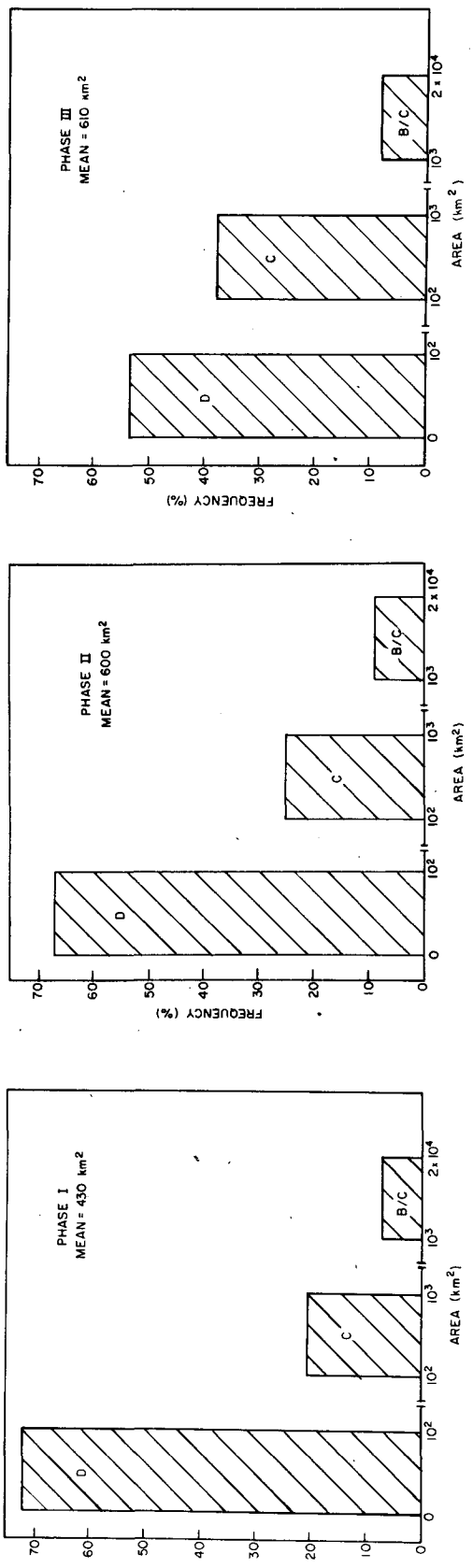


FIG. 15. Frequency of occurrence of D, C and B/C scale radar echoes during the three phases of GATE.

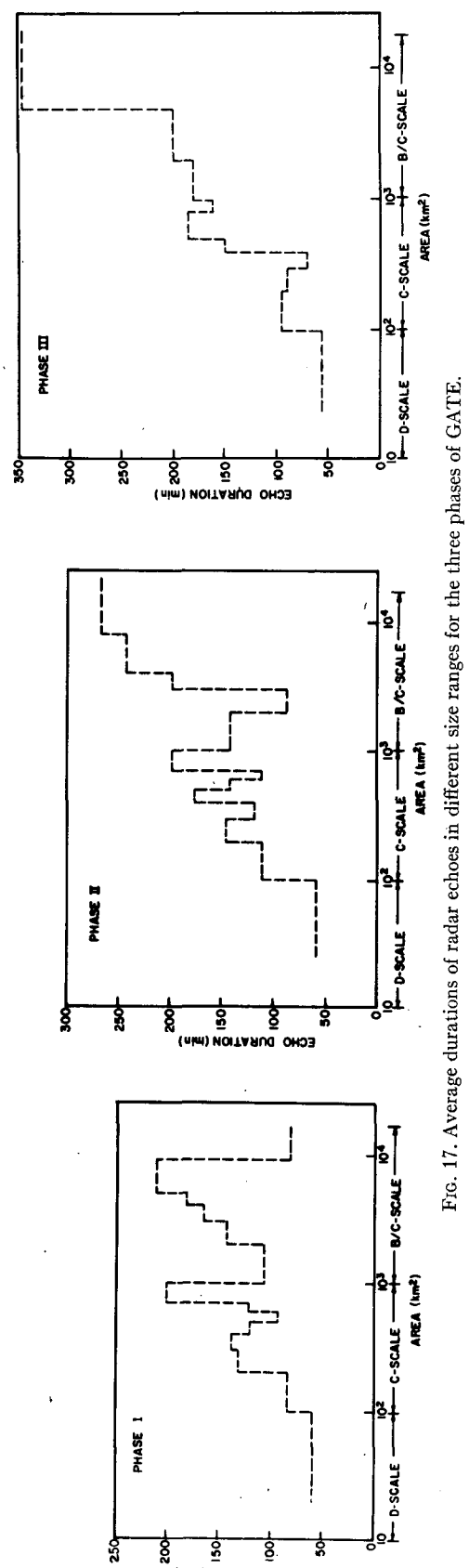


FIG. 17. Average durations of radar echoes in different size ranges for the three phases of GATE.

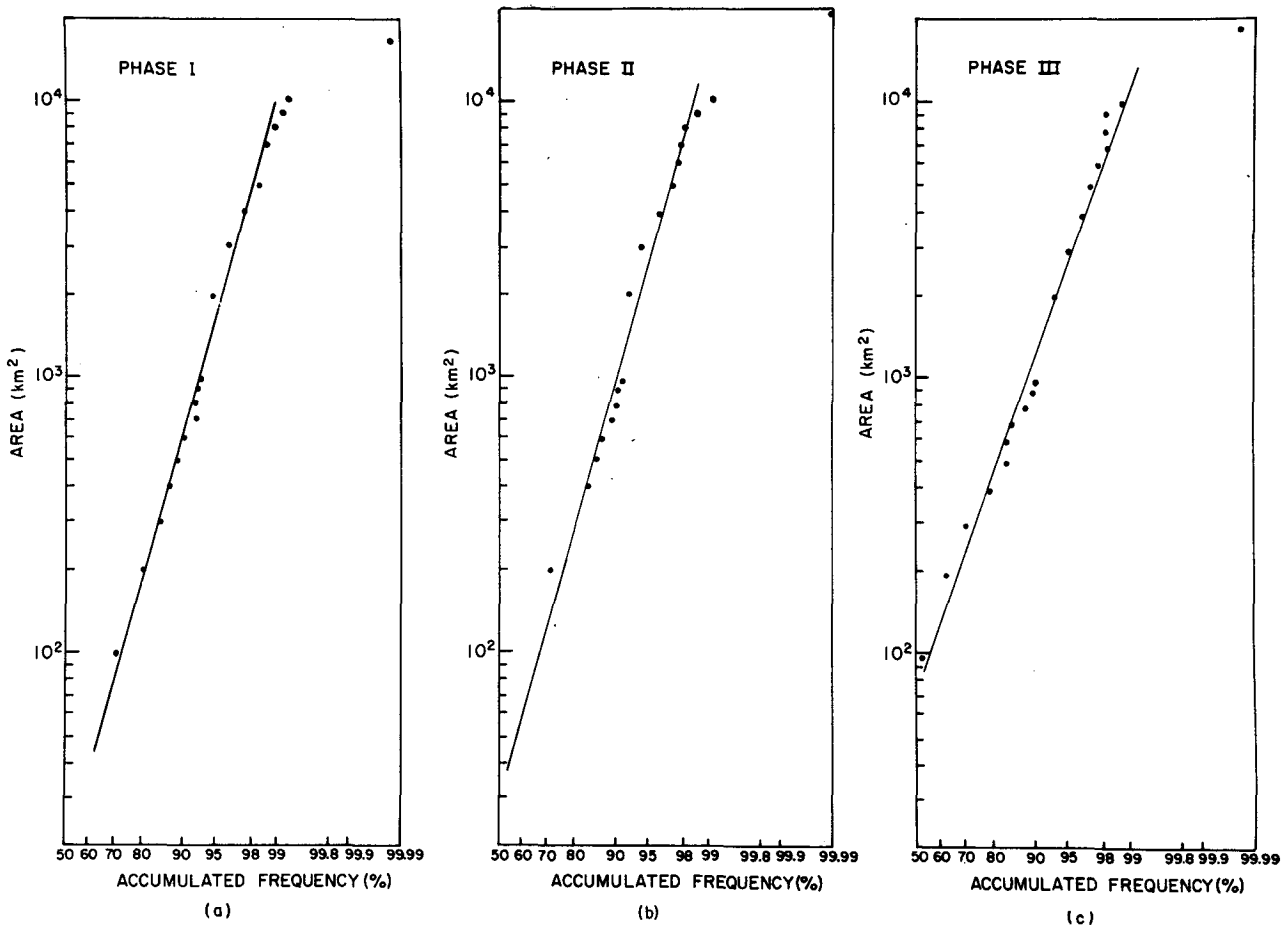


FIG. 16. Accumulated frequency distributions of areas covered by radar echoes plotted in log-probability format for the three phases of GATE. The straight lines indicate the log-normal distributions computed from the means (1.47, 1.55, 1.74) and standard deviations (0.81, 0.85, 0.86) of the logarithms of the observed echo areas in km² for Phases I, II and III, respectively.

indicated in Fig. 16 at the 5% level of significance for echoes $<10^4$ km² in area.

*b. Echo formation, dissipation and duration*

The increased frequency of C scale echoes from Phase I to Phase III, seen in Fig. 15, was accompanied by a trend of the C scale echoes to form and dissipate by mergers and splits as the summer progressed (Table 5). We interpret this trend as an indication of increased interaction of individual convective elements in more organized convective systems accompanying the increased synoptic-scale wave activity in Phase III. The formation and dissipation modes of the smaller D scale echoes changed little over the summer, suggesting that these existed rather independently of the more organized convection. The large B/C scale echoes formed and dissipated nearly always by mergers and splits throughout the summer, suggesting that these echoes were in themselves evidence of organized convection, whenever they occurred.

The relationships in Fig. 17 show that echo duration and echo area were positively correlated in each phase of GATE. Although the lifetimes of the D and C scale echoes, indicated in Fig. 17, changed little from one phase to the next, the durations of larger B/C scale echoes increased steadily through the summer. The convective regime of Phase III thus appeared to favor B/C scale echoes with long lifetimes.

The frequency distributions of echo duration (Figs. 18 and 19) were similar in all three phases of GATE. Each distribution passed the chi-square test for goodness of fit to the log-normal distributions indicated in Fig. 19 at the 5% level of significance.

*c. Echo height*

The mean maximum height attained by GATE radar echoes did not vary much over the summer (Fig. 20). From Fig. 21, it can be seen that the distribution of maximum echo height remained log-normal throughout GATE, passing the chi-square test for goodness of fit to the straight lines shown in Fig. 21 at the 5% level of significance for each phase.[3]

[3] In applying the chi-square test, the data point for the largest echo-height category, which tends to deviate from log-normality in the tail of the distribution, was ignored.

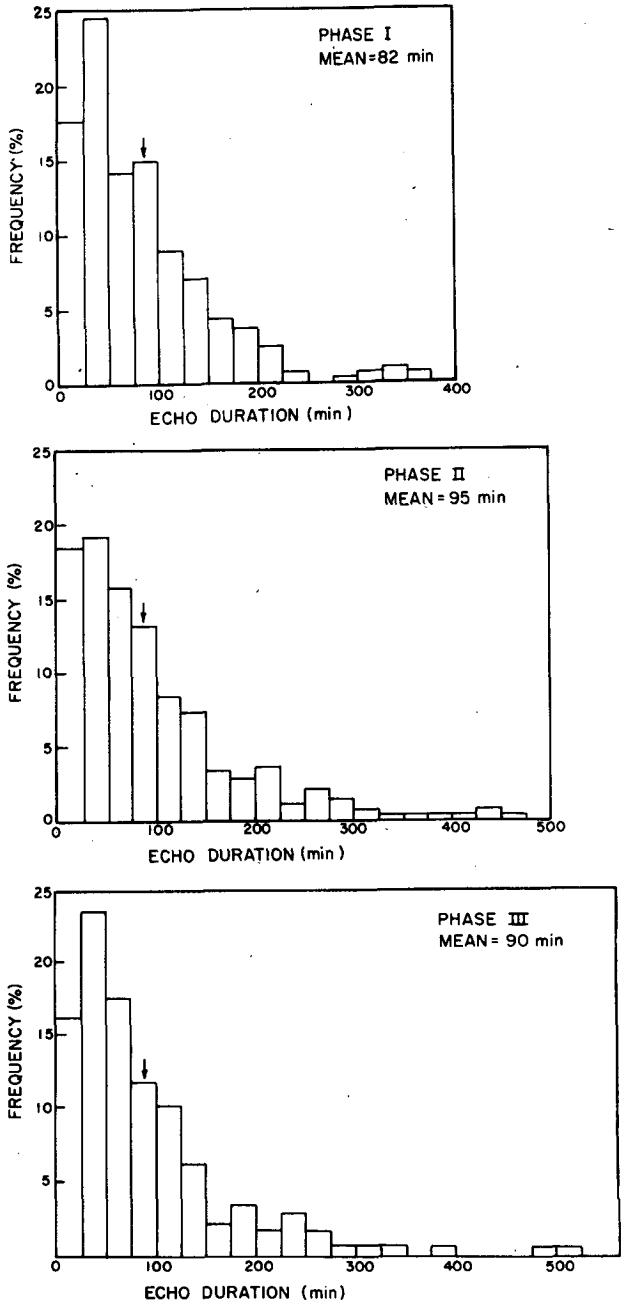


FIG. 18. Frequency distributions of radar echo durations for the three phases of GATE. Arrows indicate mean values.

The relationship between echo area ($A$) and average maximum height (AMH) for each phase of GATE is shown in Fig. 22. During each phase, there was an increase of AMH with log $A$. Phase I, however, was characterized by relatively shallow echoes in all horizontal size categories. In the transition from Phase I to Phase II, echoes of each horizontal scale increased substantially in height. However, in the transition from Phase II to Phase III, the AMH of D and C scale echoes decreased back to the level of Phase I, while the

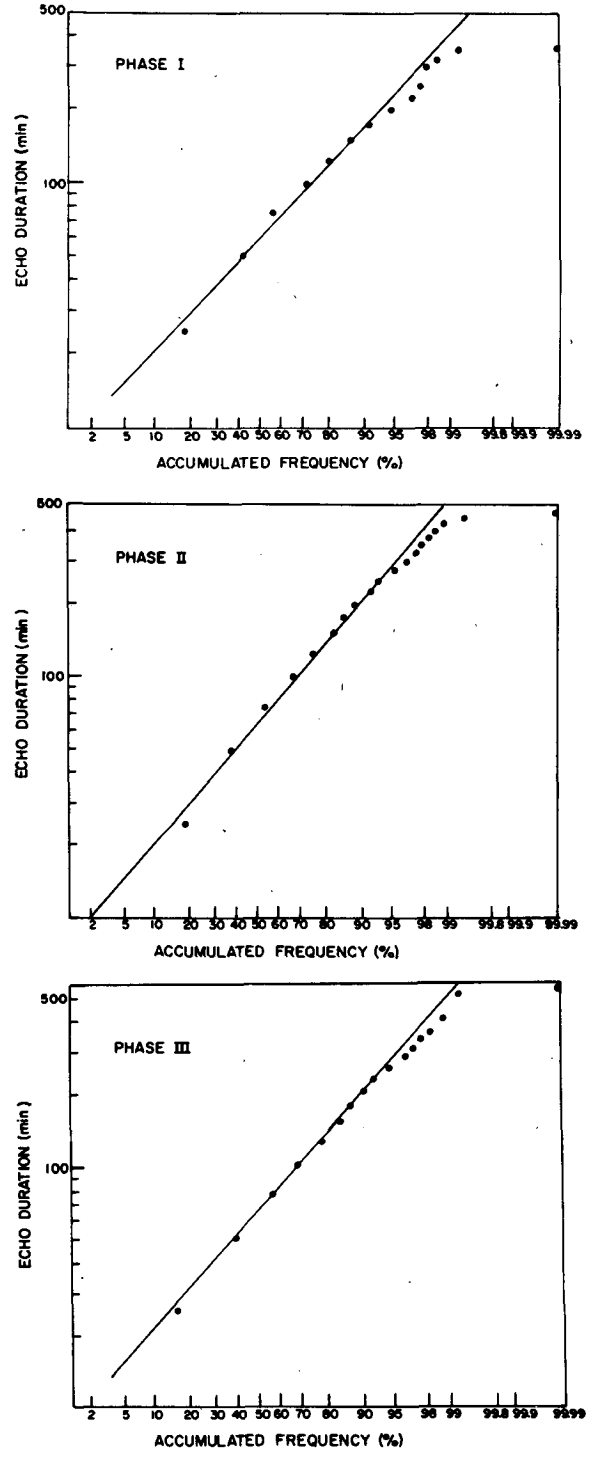


FIG. 19. Accumulated frequency distributions of radar echo durations plotted in log-probability format for the three phases of GATE. The straight lines indicate the log-normal distributions computed from the means (1.77, 1.81, 1.80) and standard deviations (0.36, 0.40, 0.38) of the logarithms of the observed echo durations in units of minutes for Phases I, II and III, respectively.

B/C scale echoes increased further in height. Thus, in Phase III the maximum heights reached in broad B/C scale cloud systems continued to increase as the summer progressed, while the smaller D and C scale echoes reversed their earlier trend and were somewhat suppressed in height during Phase III.

### *d. Echo internal structure*

The internal structure of D scale and C scale echoes appeared to change little from Phase I to Phase III of GATE (Fig. 23). However, the average number of higher intensity cores embedded in the large B/C scale

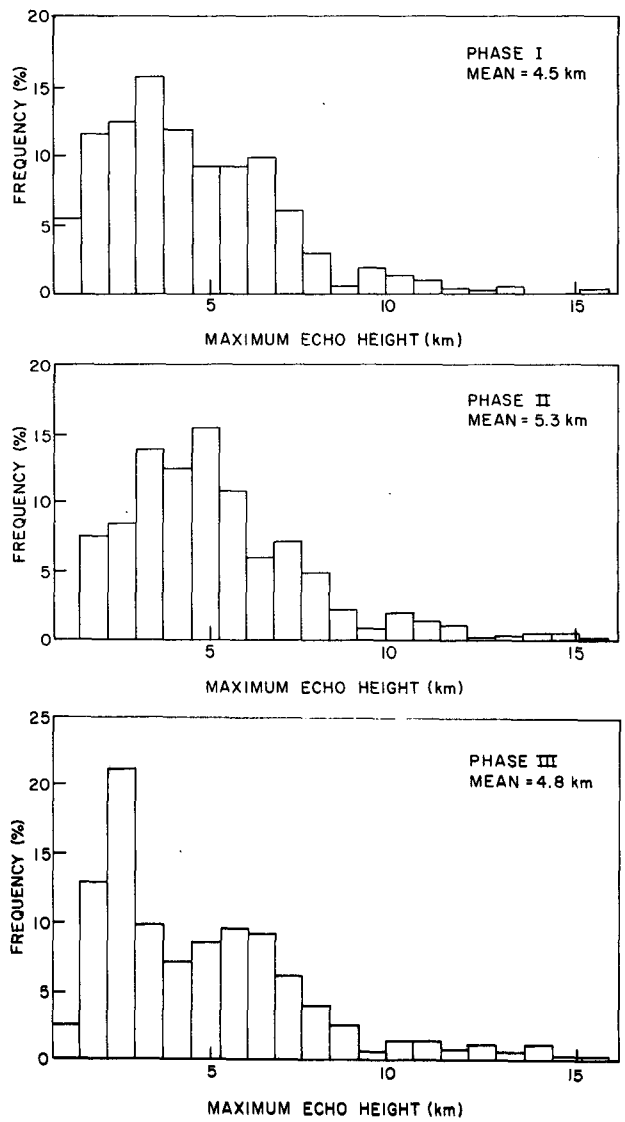


FIG. 20. Frequency distributions of the maximum heights of radar echoes observed during the three phases of GATE. Arrows indicate mean values.

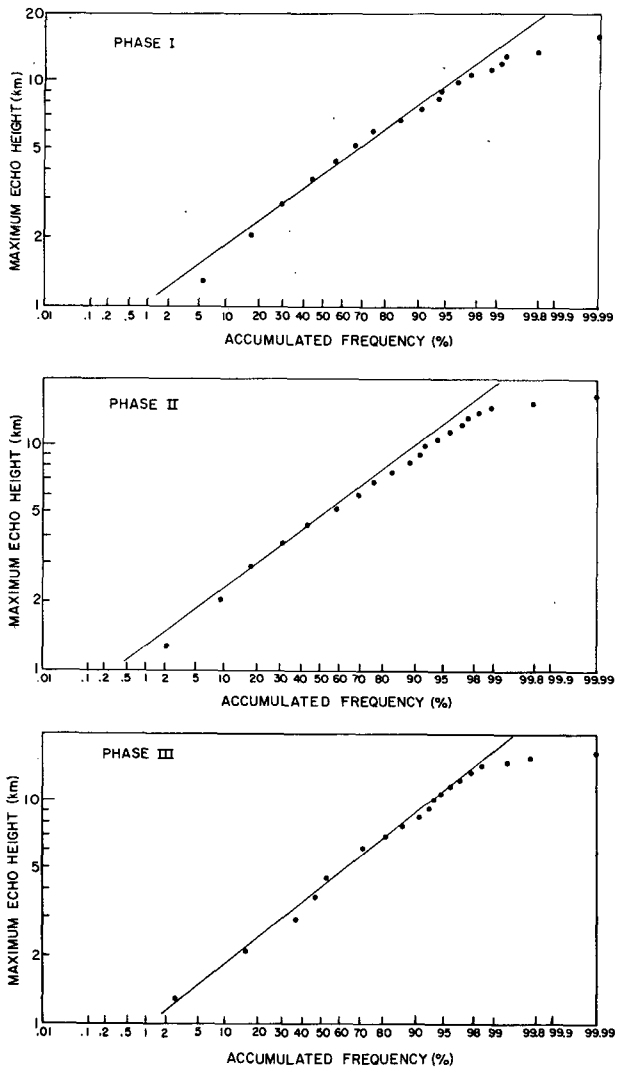


FIG. 21. Accumulated frequency distributions of the maximum heights of radar echoes plotted in log-probability format for the three phases of GATE. The straight lines indicate the log-normal distributions computed from the means (0.55, 0.61, 0.63) and standard deviations (0.17, 0.24, 0.21) of the logarithms of the observed maximum echo heights in units of km for Phases I, II and III, respectively.

echoes (specifically, those exceeding 2000 km$^2$ in area) increased progressively from one phase to the next, with the biggest increase, seen in Fig. 22, occurring between Phases II and III. Furthermore, the majority of the embedded cores in these very large echoes reached intensity levels 3 or 4 during Phase III while those in Phases I and II tended to reach only level 2. Thus, the convective regime of Phase III not only favored B/C scale echoes with longer lifetimes and greater vertical development, these large echoes contained embedded convective cores which were both more numerous and more intense.

## 5. Conclusions

The radar echoes associated with tropical convection in GATE exhibited a hierarchy of scales, dominated numerically by small, independently forming and dissipating D scale echoes ($<100$ km$^2$ in area). The area covered by radar echoes, however, was dominated by large B/C scale echoes ($>10^3$ km$^2$ in area) which tended to form and dissipate by echo mergers and splits.

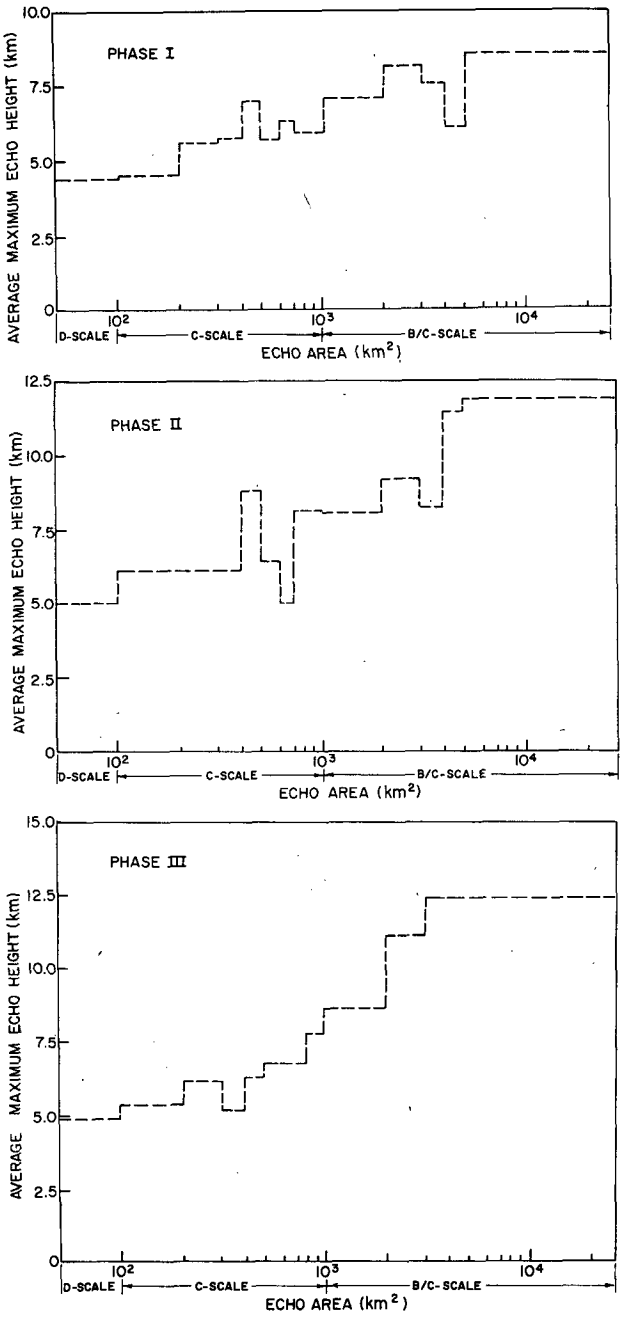


FIG. 22. Average maximum heights of radar echoes in different size ranges for the three phases of GATE.

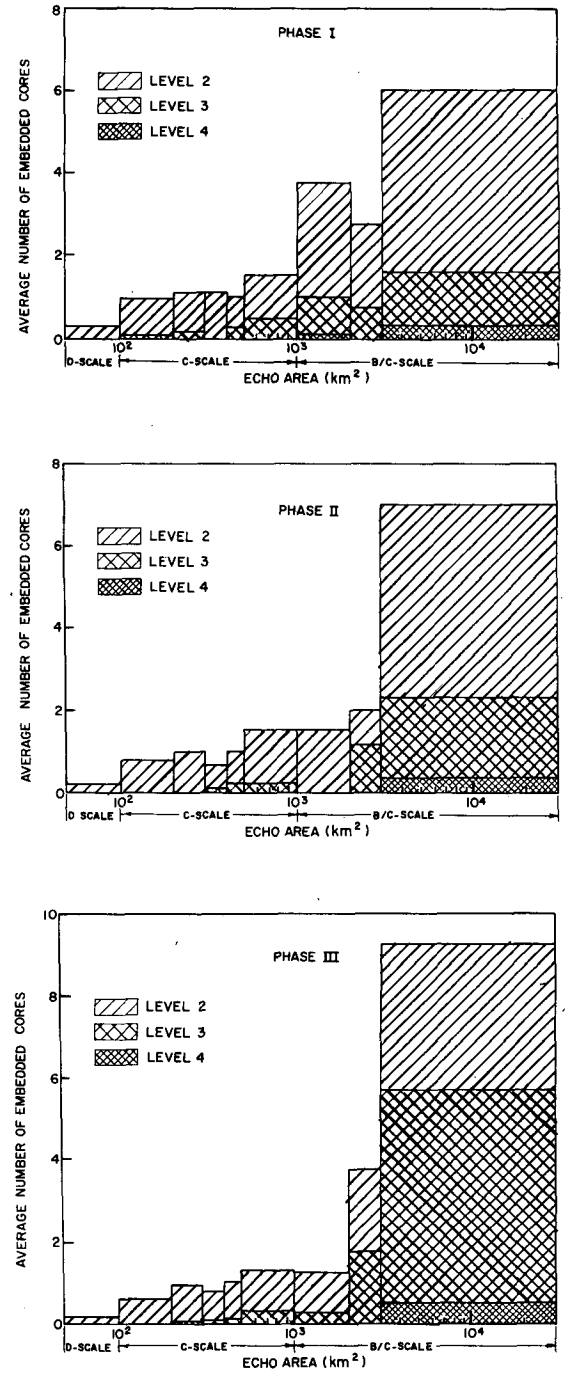


FIG. 23. Average number of embedded cores of maximum reflectivity located within radar echoes in different size ranges during the three phases of GATE. For explanation of shading scheme, see caption to Fig. 11.

The distributions of echo area, height and duration tended to be log-normal, a typical characteristic of radar echo populations noted previously by López (1976, 1977) and Biondini (1976). Echo area, height and duration were all positively correlated.

The larger echoes (C and B/C scale) had embedded cores of high-radar reflectivity. The largest B/C scale echoes thus formed protected regions, favoring the development of the most intense echo cores and the deepest convection or the more intense convection produced surrounding areas of widespread precipitation.

Radar echoes of all sizes in GATE moved slowly, except in relatively rare squall-line situations, such as those described by Houze (1975, 1976, 1977). Echoes not associated with squall lines moved with the lower tropospheric (850–700 mb) winds at typical speeds of 3–5 m $s^{-1}$. The lower tropospheric wind also apparently played a role in aligning large groups of echoes, which almost always exhibited an orientation within $\pm 25°$ of either the 700 mb wind, the 850 mb wind or a surface wind confluence line. To a lesser extent, the lower tropospheric wind may have influenced the alignment of individual elongated echoes.

The GATE convective regime changed as the summer progressed with the most notable changes occurring between mid-summer (Phase II of GATE) and late summer (Phase III of GATE). A larger proportion of C scale (100–1000 $km^2$) echoes occurred during Phase III than during Phases I and II, and the C scale echoes in Phase III tended to form less independently and more by mergers and splits than earlier in the summer. The B/C scale echoes in Phase III lasted longer, reached greater maximum heights, and their embedded echo cores were more numerous and stronger than earlier in the summer.

Our average radar echo characteristics for convection over the eastern tropical Atlantic Ocean have many features in common with the findings of IW and L for the western tropical Atlantic, especially with regard to the form of the distributions of echo area, height and duration, which all tend to be log-normal. This work provides a basic description of convective cloud population characteristics to which those concerned with the modelling and parameterization of cumulus and synoptic scale interaction can refer and serves as a background against which the representativeness of case studies of specific GATE disturbances can be judged.

Our study was based on the photographic records of the *Oceanographer* radar displays, which were the first GATE radar data available to researchers. With digital data now available from all four quantitative radars employed in GATE, we are undertaking studies in which cloud populations are represented by the distribution of rainfall among clouds of different heights. This information will serve directly as input to cloud models, such as those developed by Austin and Houze (1973), Houze (1973) and Houze and Leary (1976), to compute the vertical transports of mass, energy and momentum by the large groups of convective clouds in GATE tropical disturbances.

*Acknowledgments.* The authors had the opportunity to discuss this work with Dr. Raúl E. López on several occasions and we appreciate his interest and helpful comments. Professor Richard J. Reed and Ms. Colleen Leary read the manuscript and made helpful suggestions. Ms. Jean Dewart and Mr. Roy Brown assisted in tracking radar echoes and tabulating the data. The figures were drafted by Mrs. Kay Moore.

This work was supported by the Global Atmospheric Research Program, National Science Foundation, and the U. S. GATE Project Office under Grant ATM 74-14830 A01.

## REFERENCES

Aitchison, J., and J. A. C. Brown, 1957: *The Lognormal Distribution.* Cambridge University Press, 176 pp.

Austin, P. M., and R. A. Houze, Jr., 1973: A technique for computing vertical transports by precipitating cumuli. *J. Atmos. Sci.*, **30**, 1100–1111.

Biondini, R., 1976: Cloud motion and rainfall statistics. *J. Appl. Meteor.*, **15**, 205–224.

Houze, R. A., Jr., 1973: A climatological study of vertical transports by precipitating cumuli. *J. Atmos. Sci.*, **30**, 1112–1123.

——, 1975: Squall lines observed in the vicinity of the *Researcher* during Phase III of GATE. *Preprints 16th Conf. Radar Meteorology*, Houston, Amer. Meteor. Soc., 206–209.

——, 1976: GATE radar observations of a tropical squall line. *Preprints 17th Conf. Radar Meteorology*, Seattle, Amer. Meteor. Soc., 384–389.

——, 1977: Structure of a tropical squall-line system observed during GATE. Submitted to *Mon. Wea. Rev.*

——, and C. A. Leary, 1976: Comparison of convective mass and heat transports in tropical easterly waves computed by two methods. *J. Atmos. Sci.*, **33**, 424–429.

Hudlow, M. D., 1975a: Documentation for GATE *Oceanographer* radar film. GATE Processed and Validated Data [Available from World Data Center, National Climatic Center, Asheville, N. C.], 50 pp.

——, 1975b: Collection and handling of GATE shipboard radar data. *Preprints 16th Conf. Radar Meteorology.*, Houston, Amer. Meteor. Soc., 186–193.

ISMG (Interim Scientific and Management Group), 1972: Experiment design proposal for the GARP Atlantic Tropical Experiment. GATE Rep. No. 1., WMO–ICSU, Geneva, 188 pp.

Iwanchuk, R. M., 1973: Characteristics and distribution of precipitation areas over the tropical Atlantic. S. M. thesis, Dept. of Meteorology, MIT, Cambridge, Mass., 106 pp.

Johnson, R. H., 1976: The role of convective-scale precipitation downdrafts in cumulus and synoptic-scale interactions. *J. Atmos. Sci.*, **33**, 1890–1910.

López, R. E., 1973: Cumulus convection and larger scale circulation, II. Cumulus and mesoscale interactions. *Mon. Wea. Rev.*, **101**, 856–870.

——, 1976: Radar characteristics of the cloud populations of tropical disturbances in the northwest Atlantic. *Mon. Wea. Rev.*, **104**, 268–283.

——, 1977: The lognormal distribution and cumulus cloud populations. *Mon. Wea. Rev.* **105**, 865–872.

National Academy of Sciences, 1971: Plan for U. S. Participation in the GARP Atlantic Tropical Experiment. Report of the Ad Hoc Tropical Task Group to the U. S. Committee for the Global Atmospheric Research Program, National Research Council, Washington, D. C., 25 pp.

Ogura, Y., and H.-R. Cho, 1973: Diagnostic determination of cumulus cloud populations from observed large-scale variables. *J. Atmos. Sci.*, **30**, 1276–1286.

Pestaina-Haynes, M., and G. L. Austin, 1976: Comparison between maritime tropical (GATE and Barbados) and continental mid-latitude precipitation lines. *J. Appl. Meteor.*, **15**, 1077–1082.

Reed, R. J., D. C. Norquist and E. E. Recker, 1977: The structure and properties of African wave disturbances as observed during Phase III of GATE. *Mon. Wea. Rev.*, **105**, 317–333.

Yanai, M., S. Esbensen and J.-H. Chu, 1973: Determination of bulk properties of tropical cloud clusters from large-scale heat and moisture budgets. *J. Atmos. Sci.*, **30**, 611–627.